Available online at www.sciencedirect.com
SCIENCE DIRECT®
International Journal of Pharmaceutics 303 (2005) 132–142
international journal of pharmaceutics
www.elsevier.com/locate/ijpharm

Effect of a melt agglomeration process on agglomerates containing solid dispersions

Thomas Vilhelmsen[a], Helle Eliasen[b], Torben Schæfer[a,*]

[a] *The Danish University of Pharmaceutical Sciences, Department of Pharmaceutics, 2 Universitetsparken, DK-2100 Copenhagen, Denmark*
[b] *H. Lundbeck A/S, Research & Development, 9 Ottiliavej, DK-2500 Copenhagen Valby, Denmark*

Received 11 February 2005; received in revised form 30 June 2005; accepted 13 July 2005
Available online 1 September 2005

Abstract

The purpose was to produce solid dispersions of a poorly water-soluble drug, Lu–X, by melt agglomeration in a laboratory scale rotary processor. The effect of binder type and method of manufacturing on the dissolution profile of Lu–X was investigated. Lactose monohydrate and Lu–X were melt agglomerated with Rylo MG12, Gelucire 50/13, PEG 3000, or poloxamer 188. Either a mixture of binder, drug, and excipient was heated to a temperature above the melting point of the binder (melt-in procedure) or a dispersion of drug in molten binder was sprayed on the heated excipient (spray-on procedure). The agglomerates were characterized by DSC, XRPD, SEM, and EDX-SEM. The study showed that the agglomerates containing solid dispersions had improved dissolution rates compared to physical mixtures and pure drug. The melt-in procedure gave a higher dissolution rate than the spray-on procedure with PEG 3000, poloxamer 188, and Gelucire 50/13, whereas the opposite was found with Rylo MG12. This was explained by differences in mechanisms of agglomerate formation and growth, which were dominated by immersion with PEG 3000, poloxamer 188, and Gelucire 50/13, and by distribution and coalescence with Rylo MG12. The spray-on procedure resulted in a higher content of Lu–X in the core of the agglomerates when immersion was the dominating mechanism, and in a higher content in the agglomerate surface when distribution was dominating. The melt-in procedure resulted generally in a homogeneous distribution of Lu–X in the agglomerates. The compounds in the agglomerates were found primarily to be crystalline, and the dissolution profiles were unchanged after 12 weeks storage at 25 °C at 50% RH.

Keywords: Rotary processor; Solid dispersion; Melt agglomeration; Dissolution; EDX-mapping; Agglomerate growth mechanisms

1. Introduction

The dissolution profile of a drug with poor water solubility might be improved by formulating it as a solid dispersion. A solid dispersion consists of a drug dispersed in a solid carrier matrix. The dispersed drug

* Corresponding author. Tel.: +45 35 306 000; fax: +45 35 306 030.
E-mail address: ts@dfuni.dk (T. Schæfer).

0378-5173/$ – see front matter © 2005 Elsevier B.V. All rights reserved.
doi:10.1016/j.ijpharm.2005.07.012

in the carrier might be crystalline or amorphous. The term solid solution is used for drugs that are molecularly dispersed in the solid carrier. However, whether it is a solid dispersion or a solid solution it is supposed to be the greatly enhanced surface area of the drug that improves the dissolution profile (Serajuddin, 1999).

By choosing the right carrier, the dissolution profile can be further improved. Water-soluble carriers have been shown to give a fast dissolution of drug (Passerini et al., 2002; Seo et al., 2003). Furthermore, it has been shown that the dissolution profile can be improved if the carrier has surface active or self-emulsifying properties (Damian et al., 2000; Passerini et al., 2002; Serajuddin et al., 1988; Khoo et al., 2000; Seo et al., 2003).

Solid dispersions have in laboratory scale been prepared by adding and to some extent dissolving the drug in the molten carrier followed by solidification and pulverization of the formed solid dispersion, by dissolving the drug and the carrier in a common organic solvent followed by evaporation of the solvent, or by dissolving the drug in an organic solvent, which is added to the molten carrier (Serajuddin, 1999). The problems related to these manufacturing methods are difficulties in manufacturing, scale-up, formulation into dosage forms, poor reproducibility, as well as stability (Serajuddin, 1999). Therefore, it would be an advantage if the formation of a solid dispersion could be achieved using a reproducible process, which easily can be implemented in an industrial scale.

A suitable process could be melt agglomeration since studies have shown that it is possible in a laboratory scale high shear mixer to produce agglomerates containing solid dispersions by a melt agglomeration process where the binder also acts as a carrier (McTaggart et al., 1984; Kinget and Kemel, 1985; Zhou et al., 1996; Voinovich et al., 2000; Passerini et al., 2002; Gupta et al., 2002; Seo et al., 2003).

The solid dispersions made by melt agglomeration in high shear mixers have either been made by adding the molten binder containing the drug to the heated excipients (Ford and Rubinstein, 1980; Kinget and Kemel, 1985; Gupta et al., 2002; Seo et al., 2003), by adding the molten binder to a heated mixture of drug and excipients (Zhou et al., 1996; Passerini et al., 2002), or by heating a mixture of the drug, binder and excipients to a temperature within or above the melting range of the binder (McTaggart et al., 1984; Voinovich et al., 2000; Seo et al., 2003).

A rotary processor has been shown to be an alternative equipment for melt agglomeration (Vilhelmsen et al., 2004). The rotary processor might be preferable to the high shear mixer for manufacturing solid dispersions by melt agglomeration because it is easier to control the temperature and because a higher binder content can be incorporated in the agglomerates (Vilhelmsen et al., 2004).

The hypothesis for the present work was that a melt agglomeration process in a rotary processor could be used to prepare solid dispersions. The purpose of this study was to test this hypothesis by investigating the effect of the binder addition procedure for four different meltable binders on the dissolution profile of a drug with poor water solubility.

2. Materials and methods

2.1. Materials

Lactose 350 mesh (α-lactose monohydrate, DMV, The Netherlands) was used as filler. Different sieve fractions from four meltable binders/carriers were used for the melt-in procedure, the sieve fraction 355–750 μm from grinded Rylo^{TM} MG12 beads (monoglyceride with lauric acid, Danisco Emulsifiers, Denmark), the sieve fraction 315–630 μm from grinded Gelucire® 50/13 beads (mixture of glycerides and PEG esters of fatty acids, Gattefossé, France), the sieve fraction 250–500 μm from polyethylene glycol 3000 powder (Clariant, Germany), and the sieve fraction 0–315 μm from grinded poloxamer 188 micropearls (BASF, Germany). Unfractionated binders/carriers were used for the spray-on procedure. As the active pharmaceutical ingredient a substance called Lu–X (H. Lundbeck, Denmark) was used. Lu–X is practically insoluble in water with an intrinsic solubility of 0.003 μg/ml. Lu–X is a weak base with an estimated pK_a-value of 9. Therefore, the aqueous solubility of Lu–X increases with decreasing pH.

2.2. Methods

2.2.1. Characterization of materials

The particle size distributions by volume of the lactose, the sieve fractions of the binders, and Lu–X were determined in triplicate by a Malvern Mastersizer S

laser diffraction particle sizer (Malvern Instruments, UK) fitted with a dry powder feeder operating at 3 bar. The span was calculated as the difference between the volume diameters at the 90 and 10% points relative to the volume median diameter.

Both the BET multipoint surface area and the Blaine specific surface area were determined for the lactose and Lu–X. The BET multipoint surface area was determined in duplicate by a Gemini 2375 Surface Area Analyzer (Micromeritics, USA). The Blaine specific surface area was determined in duplicate by a Ph. Eur. Blaine Gaspermeameter (European Pharmacopoeia, 2002).

The pycnometric densities of the lactose, the meltable binders, and Lu–X were determined in duplicate by an AccuPyc 1330 gas displacement pycnometer (Micromeritics, USA) using helium purge.

The melting ranges and the melting peak temperatures of the lactose, the binders, and Lu–X were estimated in triplicate by a Perkin-Elmer DSC 7 differential scanning calorimeter (Perkin-Elmer, USA). Samples of about 4 mg were sealed in 40 μl aluminum pans with holes and scanned at a heating rate of 10 °C/min. DSC scans were performed on mixtures of Lu–X and each of the binders in different ratios and about 4 mg were scanned at a heating rate of 5 °C/min. The mixtures were prepared by dissolving Lu–X and the binder in ethanol followed by evaporation of the solvent at ambient conditions.

The densities of the molten binders were determined in triplicate at 60 and 70 °C as previously described (Eliasen et al., 1998).

The viscosities of the molten binders were determined in duplicate by a RV20 Rotovisco (Haake, Germany) with a NV sensor system and a measuring system M. The viscosities were determined at 60 and 70 °C as the slope of the linear part of the obtained flow curve.

The solubilities of Lu–X in the binders were determined in duplicate colorimetrically at 280 nm using a Perkin-Elmer Lambda 14P spectrophotometer (Perkin-Elmer, USA) by measuring the concentration of Lu–X in the clear saturated supernatant of the sedimentated dispersion of Lu–X in the molten binders kept at 60 °C in a thermostat water bath (Jouan Nordic, Denmark).

The droplet size distributions by volume of the dispersion of molten binders and Lu–X were determined at process conditions in duplicate by a Malvern 2600 C laser diffraction particle sizer (Malvern Instruments, UK). The nozzle was placed perpendicularly 133 mm from the lens, and the nozzle orifice was placed perpendicularly 50 mm from the laser beam and adjusted vertically to the same height as the laser beam.

2.2.2. Agglomeration equipment

The melt agglomeration experiments were performed in a rotary processor (Glatt GPCG-1, Glatt, Germany) fitted with a friction plate of 28 cm in diameter and a surface consisting of elevated cubes in a cross-hatched pattern. An additional temperature sensor (Greisinger Electronic, Germany) was inserted, and readings were recorded manually as previously described (Vilhelmsen et al., 2004) and used as the product temperature. The rotary processor was connected to a standard personal computer (Hewlett–Packard, USA), which monitored and recorded the process data. For spray-on experiments, the standard Schlick pneumatic atomizer model 970/0-S21 (Glatt, Germany) was used with an orifice of 1.2 mm and an air dome setting of 2. The nozzle was placed with the spray tangentially to the moving powder. The atomizing air was heated to 160 °C by an electrically heated tube (Isopad, Germany). A pressure vessel (Alloy, USA) with a capacity of 7.5 l heated to 75 °C delivered the molten dispersion to the nozzle through a tube (Hillesheim, Germany) with an internal diameter of 3 mm electrically heated to 80 °C.

2.2.3. Agglomeration procedure

2.2.3.1. Formulations. The formulations are presented in Table 1. The concentration of Lu–X was 25% m/m of the amount of binder in all experiments. The binder concentration was 22% v/m at 60 °C of the total amount of lactose and Lu–X. However, the binder concentration had to be lowered to 20% v/m in the spray-on experiments with Rylo due to uncontrollable growth of the agglomerates.

2.2.3.2. Preheating. Before all the experiments, the rotary processor was preheated to a product temperature of 50 °C. During the preheating of the rotary processor and the massing time, the fluidizing airflow was set to 70 m^3/h, the inlet fluidizing air temperature to 70 °C, the fluidizing air gap pressure drop to 2000 Pa, and the friction plate rotation speed to 1000 rpm.

Table 1
Composition of formulations used in the rotary processor

Meltable binder/carrier	Binder addition procedure[a]	Binder/carrier (g)	Lactose (g)	Lu–X (g)
Rylo MG12	Melt-in	147.8	663.0	37.0
Rylo MG12	Spray-on	134.4	666.4	33.6
Gelucire 50/13	Melt-in and spray-on	154.0	661.5	38.5
PEG 3000	Melt-in and spray-on	167.9	658.0	42.0
Poloxamer 188	Melt-in and spray-on	164.8	658.8	41.2

[a] Melt-in: solid binder particles are added. Spray-on: dispersions of Lu–X in molten binder are added.

2.2.3.3. Massing time. The start of massing time was defined as the point where the product temperature in the melt-in experiments increased rapidly around the melting range of the binder (Table 2). The length of the massing time (Table 2) was chosen in order to obtain a sufficient amount of agglomerates within the size fraction 500–630 μm for all the binders.

2.2.3.4. Melt-in procedure. When the melt-in procedure was applied, the lactose, the binder, and Lu–X were manually mixed for 20 s before they were placed at the centre of the friction plate in the preheated rotary processor. After the fluidizing airflow was started, the fluidizing air gap pressure drop was adjusted, and finally the rotation of the friction plate was started. When the specified product temperature (Table 2) was reached, the timing of the massing time was started.

2.2.3.5. Spray-on procedure. When the spray-on procedure was applied, the binder was melted in an oven (Termaks, Norway) at 80 °C. Approximately 1 h before the process, the Lu–X was added to the molten binder, mixed manually, and stored in the oven at 80 °C. Then, the lactose was weighed and placed at the centre of the friction plate in the preheated rotary processor, and the process was started as described above. Shortly before commence of spraying, the molten dispersion was stirred and added to the pressure vessel. When the specified product temperature (Table 2) was reached, the spraying of the dispersion of molten binder and Lu–X into the lactose was begun, and the timing of the massing time was started. After spraying of the dispersion, the atomization air pressure was kept at a cleaning pressure of 1 bar. The spraying of the dispersion lasted around 0.6, 0.9, 1.6, and 4.6 min for Rylo, Gelucire, PEG, and poloxamer, respectively.

2.2.3.6. Cooling. For both procedures, a valve with an internal diameter of 60 mm conducting unheated air of room temperature into the container was opened at the end of massing time, and the cooling was started. During the cooling, the fluidizing airflow was set to approximately 100 m^3/h and the friction plate rotation speed to 500 rpm. When the product temperature was below the melting range of the binder, the rotary processor was stopped, and the product was removed and weighed.

2.2.4. Agglomerate characterization

2.2.4.1. Storage. One day after each experiment, a representative sample of agglomerates was stored at 25 °C and 50% RH in a climate cabinet (Termaks, Norway), and the rest of the product was stored protected from light at ambient conditions.

2.2.4.2. Dissolution studies. The dissolution tests were carried out in triplicate in a Bio-Dis Extended Release Tester (VanKel Industries, Inc., USA) con-

Table 2
Fixed values for process parameters for different binders

Binder/carrier	Massing time start (°C)	Massing time for melt-in (min)	Massing time for spray-on (min)	Atomization air pressure (bar)	Pressure in heated pressure dome (bar)
Rylo MG12	58.0	7.2	2.4	1.0	2.0
Gelucire 50/13	46.0	16.5	5.0	1.0	2.0
PEG 3000	60.0	9.5	2.2	3.0	2.0
Poloxamer 188	56.5	20.5	13.5	3.0	4.0

nected to a HP8452A Diode Array Spectrophotometer (Hewlett–Packard, Germany). The dissolution temperature was 37 °C, and the sample tubes moved with 20 dips per min in a dissolution volume of 275 ml of 10^{-4} M hydrochloric acid. An amount of agglomerates from the size fraction 500–630 μm, physical mixtures, or pure Lu–X corresponding to approximately 7 mg of Lu–X was transferred to the sample tubes. Samples of dissolution medium were transferred to the spectrophotometer and back to the dissolution vessel through tubes at intervals of 2 min, and the concentration of Lu–X was measured at 256 nm. Dissolution studies were performed on the agglomerates 1 day after production and on agglomerates stored in the climate cabinet at 1, 4, and 12 weeks after production.

2.2.4.3. Lu–X concentration. The total concentration of Lu–X in agglomerates from the size fraction 500–630 μm was determined in triplicate at 280 nm using a Perkin-Elmer Lambda 14P spectrophotometer (Perkin-Elmer, USA). Around 20 mg of agglomerates were dissolved in ethanol and filtered through a membrane filter (cellulose acetate, pore size 0.45 μm) before measuring at the spectrophotometer.

2.2.4.4. Differential scanning calorimeter. Differential scanning calorimetry measurements on agglomerates from the size fraction 500–630 μm were carried out using a Perkin-Elmer DSC 7 differential scanning calorimeter (Perkin-Elmer, USA). Samples of about 4 mg were sealed in 40 μl aluminum pans with holes and scanned between 30 and 240 °C at a heating rate of 10 °C/min.

2.2.4.5. X-ray diffraction. Diffraction patterns were obtained on agglomerates from the size fraction 500–630 μm on a STOE STADI-P diffractometer (STOE, Darmstadt, Germany). Cu Kα-1 (λ = 1.540598 Å) radiation was used with a germanium monochromator. The patterns were collected with a voltage of 40 kV and a current of 45 mA. The step width was 0.1°, and the counting time was 75 s/step.

2.2.4.6. Scanning electron microscopy. Images of the size fraction 500–630 μm were taken by a scanning electron microscope (SEM) (JSM 5200, JEOL, Japan). The agglomerates were fixed with carbon double adhesive tape and sputtered with gold (E5200 Auto Sputter Coater, BioRad, UK) for 120 s before microscopy.

2.2.4.7. Scanning electron microscopy—energy dispersive X-ray. Agglomerates from the size fraction 500–630 μm were split through the centre with a scalpel, fixed with carbon double adhesive tape, and coated with fine particles of carbon from a spray (Kontakt Chemie, Denmark). The samples were then analyzed in a Leica Stereoscan 360 scanning electron microscope (Leica Microsystems, Inc., USA) with a Pentafet Link energy dispersive X-ray (Oxford Instruments, UK). Chloride was used as an indicator of Lu–X.

2.2.5. Experimental design

Four binders were used in combination with two binder addition procedures (melt-in or spray-on). All experiments were performed in duplicate giving a total of 16 experiments. All experiments with the same binder were performed in a random order on the same day, and the order of the binders was chosen randomly.

3. Results and discussion

3.1. Material properties

In Table 3, it can be seen that all four binders have rather narrow particle size distributions. This is because only a certain fraction of the binder particles was used for the melt-in experiments (Section 2.1). In Table 4, the span value for the droplet size distributions of the atomized dispersions is increasing at higher dispersion viscosities because it was difficult to obtain a uniform spray when increasing the dispersion viscosity.

When Lu–X was added to the binders in a concentration of 25% m/m, the viscosities of the binders became increased approximately two-fold (Table 4).

Furthermore, Table 4 shows that Lu–X has the highest solubility in Rylo and a much lower and similar solubility in the three other binders.

3.2. Preliminary investigations

Phase diagrams were constructed from DSC scans of solid mixtures of each of the binders and Lu–X. Since a ratio of Lu–X dissolves in the binder during the DSC scan, the phase diagram can be used to predict the sol-

Table 3
The physical properties of the solid materials

Material	Particle sizes		BET multipoint surface area (m^2/g)	Blaine specific surface area (m^2/g)	Pycnometric density (g/ml)	Melting (°C)	
	$D_{(v, 0.5)}$ (μm)	Span				Range	Peak
Lactose	33	2.43	0.78	0.37	1.54	211–221	218
Lu–X	30	1.78	0.51	0.27	1.25	221–226	225
Rylo MG12	395	1.62	–	–	1.08	54–58	57
Gelucire 50/13	405	1.38	–	–	1.13	41–46	44
PEG 3000	388	0.98	–	–	1.23	57–61	59
Poloxamer 188	238	1.20	–	–	0.97	53–55	54

Table 4
The physical properties of the molten materials

Binder/carrier	Droplet sizes of atomized dispersions		Molten binder density (g/ml)		Binder viscosity (mPa/s)		Dispersion viscosity (mPa/s)		Solubility of Lu–X at 60 °C (mg/g)
	$D_{(v, 0.5)}$ (μm)	Span	60 °C	70 °C	60 °C	70 °C	60 °C	70 °C	
Rylo MG12	88	1.73	0.96	0.95	36	24	68	43	146
Gelucire 50/13	87	1.78	1.00	1.00	72	53	133	96	8
PEG 3000	65	2.40	1.09	1.09	267	194	476	343	11
Poloxamer 188	71	2.21	1.07	1.06	2009	1450	3870	2741	6

ubility of Lu–X in the binder. The phase diagram for Rylo showed that the solubility of Lu–X in this binder was around 50% m/m. The phase diagrams for Gelucire, PEG, and poloxamer looked alike and showed that Lu–X had a maximum solubility of around 5% m/m in these three binders. This difference in solubility is confirmed by the solubility results presented in Table 4.

To obtain agglomerates of the desired size from the melt-in experiments, it was necessary to use different size fractions of different binders (Section 2.1). Furthermore, to obtain agglomerates of the desired size from the spray-on experiments, different droplet sizes had to be used for different dispersions. Therefore, the settings for the nozzle system were different for the dispersions (Table 2).

3.3. Thermal analysis

To characterize the physical state of the components in the agglomerates, DSC curves were obtained from agglomerates and the pure components. DSC curves obtained from agglomerates produced with Gelucire, PEG, and poloxamer showed similar characteristics. In Fig. 1, it can be seen that the characteristic peaks of the binders are easily identified in the DSC curve of the agglomerates suggesting that the binders are present in the same physical state after the melt agglomeration process as before. No characteristic melting peak of the Lu–X can be identified in the DSC curves obtained from agglomerates. Therefore, it was not possible on the basis of the thermal analysis to determine in which physical state Lu–X is present in the agglomerates produced by melt agglomeration.

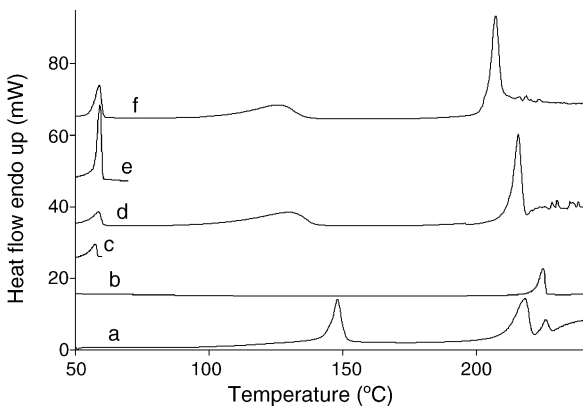

Fig. 1. DSC curves of (a) lactose, (b) Lu–X, (c) Rylo, (d) agglomerates produced by the melt-in procedure with Rylo, (e) PEG, and (f) agglomerates produced by the melt-in procedure with PEG.

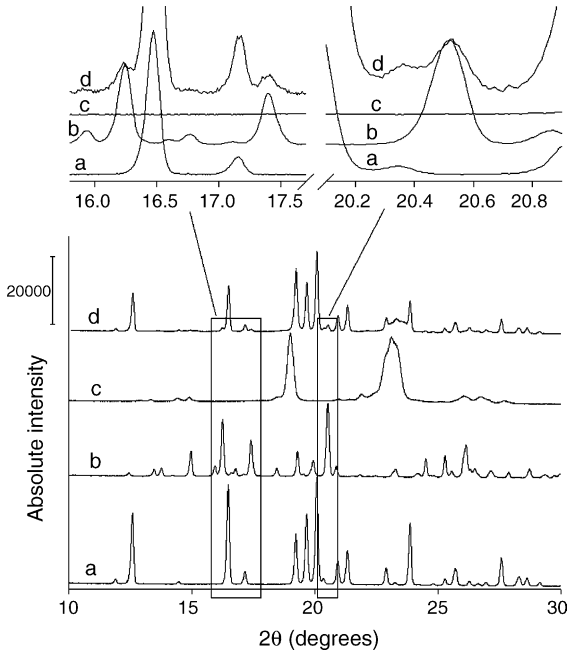

Fig. 2. X-ray powder diffraction patterns of (a) lactose, (b) Lu–X, (c) PEG, and (d) agglomerates produced by the melt-in procedure with PEG.

3.4. X-ray powder diffractograms

X-ray powder diffraction was performed on agglomerates and the pure compounds to determine the physical state of Lu–X and to complement the findings from the thermal analysis. As Fig. 2 shows, both pure lactose and pure Lu–X are primarily crystalline seen by the sharp and intense peaks. PEG (Fig. 2), Rylo, and poloxamer were also found to be primarily crystalline. Gelucire exhibited only some crystallinity because the diffractogram showed amorphous regions together with two sharp and intensive peaks. The X-ray powder diffractograms obtained from the agglomerates indicate that the physical state of the compounds was unaltered after the melt agglomeration process compared to the pure compounds.

3.5. Dissolution studies

Dissolution profiles were obtained with pure Lu–X, physical mixtures of the compounds, and agglomerates. Only dissolution profiles from one of the duplicate experiments are presented in Fig. 3 since the duplicate

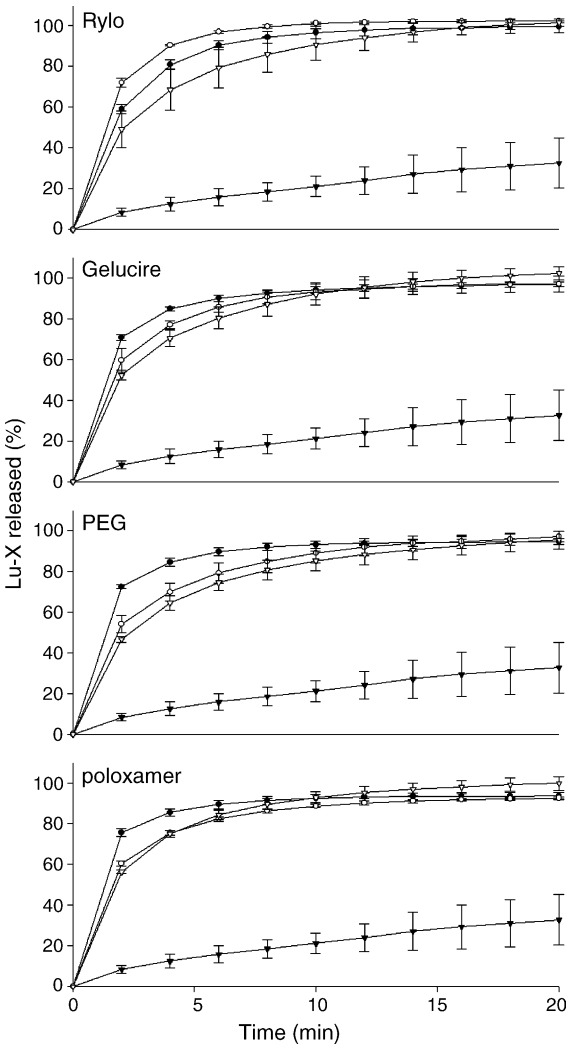

Fig. 3. Dissolution profiles of agglomerates 1 day after production containing different binders: (◯) spray-on procedure, (●) melt-in procedure, (▽) physical mixture, and (▼) pure Lu–X. The vertical bars denote the standard deviation of the triplicate determination.

dissolution profiles were found to be nearly identical. The % released in Fig. 3 is expressed as the percentage of the estimated content. The amount of Lu–X in the samples applied for the dissolution studies corresponds to approximately 17% of the solubility in hydrochloric acid at a pH value of 4 at 22 °C.

From SEM images, the surface morphology and shape of agglomerates produced with the same binder were found to be comparable regardless of the binder addition procedure.

It is seen that pure Lu–X has a markedly lower dissolution rate compared with the dissolution rates obtained with agglomerates and physical mixtures (Fig. 3) indicating that the meltable binder enhances the dissolution rate.

The highest dissolution rates from physical mixtures are obtained when the binder is Gelucire and poloxamer. This is probably due to the surface activity of these two compounds (Serajuddin et al., 1988; Passerini et al., 2002; Seo et al., 2003). The dissolution rate of the physical mixture containing Rylo is somewhat slower, and the slowest dissolution rate is from the physical mixture containing PEG.

The dissolution rates obtained from agglomerates produced by the two binder addition procedures are higher than or similar to the dissolution rates obtained from the corresponding physical mixtures.

Fig. 3 shows that the melt-in procedure gives a higher dissolution rate than the spray-on procedure for agglomerates produced with Gelucire, PEG, and poloxamer. The difference between melt-in and spray-on is less for Gelucire than for the two latter. On the contrary, for Rylo a higher dissolution rate is obtained when the spray-on procedure is applied. These differences can be explained by differences in agglomerate formation and growth mechanisms, which will be discussed in Section 3.6. However, the highest dissolution rate that was obtained for each of the binders is seen to be similar.

The dissolution profile obtained from agglomerates stored for up to 12 weeks was found unchanged compared with the dissolution profile obtained from agglomerates 1 day after production.

3.6. Mechanisms of agglomerate formation and growth

Agglomerate formation and growth in a melt agglomeration process have been described by either a distribution mechanism or an immersion mechanism (Schæfer and Mathiesen, 1996; Schæfer et al., 2004). By the distribution mechanism, the molten binder particles are distributed on the surface of the solid particles giving rise to agglomerate formation by coalescence of the wetted particles followed by an agglomerate growth by coalescence between the initial agglomerates. By the immersion mechanism, agglomerate formation occurs by an immersion of the solid particles in the surface of the molten binder particles, and further immersion of solid particles will give rise to an agglomerate growth. If the binder particle size is small compared to the solid particles, the viscosity is low, and/or the shearing forces are high then the distribution mech-

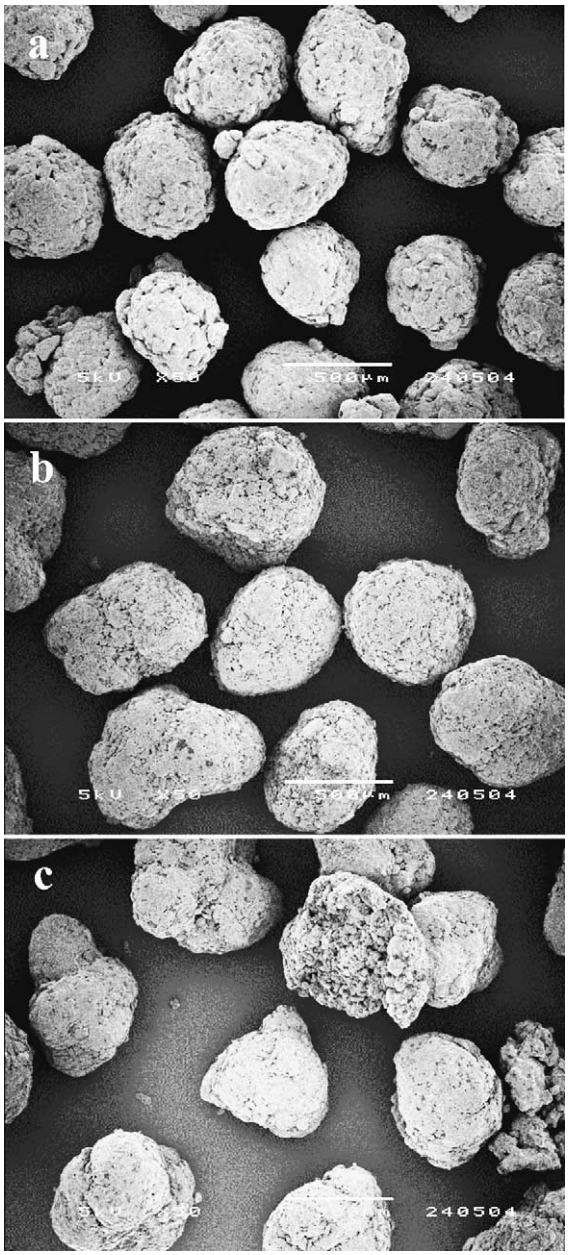

Fig. 4. SEM images of agglomerates produced with (a) PEG by the melt-in procedure, (b) Rylo by the melt-in procedure, and (c) Rylo by the spray-on procedure.

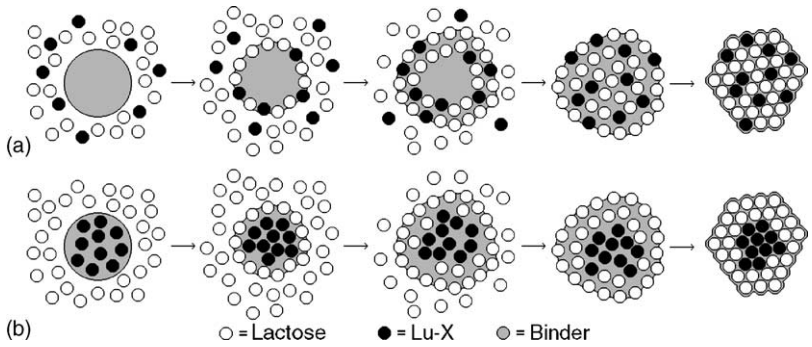

Fig. 5. Distribution of Lu–X particles during agglomerate formation and growth by the immersion mechanism for (a) the melt-in procedure and (b) the spray-on procedure.

anism is promoted, whereas the immersion mechanism is promoted by the opposite (Schæfer and Mathiesen, 1996). In practice, it might sometimes be difficult to decide whether the agglomerates have been formed by distribution or by immersion since both mechanisms might be active simultaneously due to the presence of solid particles as well as binder particles of different sizes. However, one of the mechanisms will normally be dominant.

SEM images indicate that the agglomerate formation and growth are dominated by immersion for agglomerates produced with PEG (Fig. 4a), Gelucire, and poloxamer and by distribution and coalescence with Rylo (Fig. 4b and c). Fig. 4a shows agglomerates that most likely have been formed from a single binder particle by immersion, whereas Fig. 4b and c show agglomerates that to a larger extent have been formed by coalescence between smaller agglomerates. This is in accordance with the lower viscosity of Rylo (Table 4), which will promote the distribution mechanism.

Fig. 5 illustrates that the intragranular distribution of Lu–X particles will depend on the binder addition procedure if the immersion mechanism dominates. The melt-in procedure will result in agglomerates containing Lu–X particles distributed randomly throughout the agglomerates (Fig. 5a). The spray-on procedure, on the other hand, will result in a core of Lu–X particles in the agglomerates (Fig. 5b) since the Lu–X particles are dispersed in the binder droplets before the lactose particles become immersed. Therefore, if the immersion mechanism is dominating, the spray-on procedure gives a lower dissolution rate since the Lu–X is in the core of the agglomerate. This explains the higher dis-

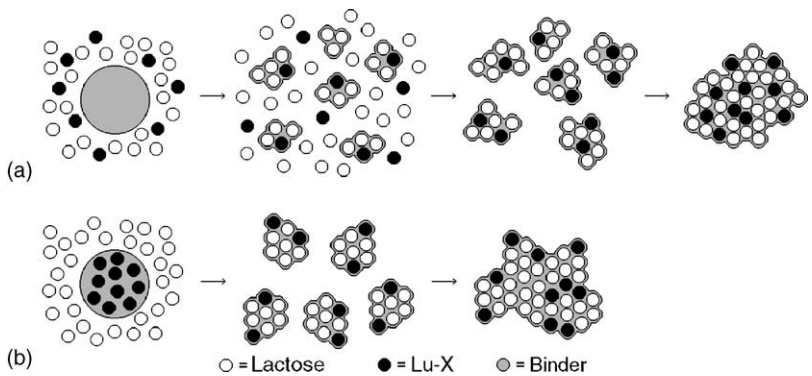

Fig. 6. Distribution of Lu–X particles during agglomerate formation and growth by the distribution mechanism for (a) the melt-in procedure and (b) the spray-on procedure.

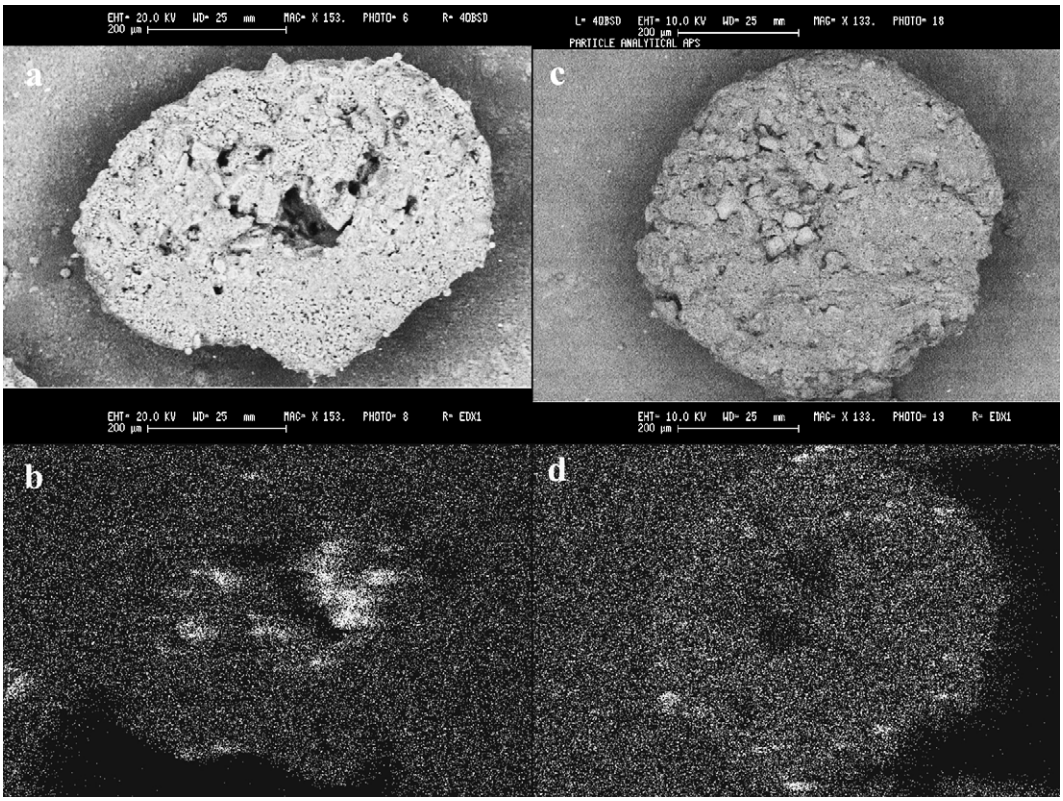

Fig. 7. SEM images (a and c) and the corresponding elemental maps of chloride (Lu–X) (b and d) of the cross-section of agglomerates produced with poloxamer (a and b) and Rylo (c and d) by the spray-on procedure.

solution rate seen from agglomerates produced by the melt-in procedure than by the spray-on procedure with Gelucire, PEG, and poloxamer (Fig. 3).

Fig. 6 illustrates the effect of the binder addition procedure on the intragranular distribution of the Lu–X particles if the distribution mechanism dominates. Again, the melt-in procedure will result in a random distribution of Lu–X (Fig. 6a). The spray-on procedure might give rise to a higher content of Lu–X in the agglomerate surface, because the Lu–X during the spraying is distributed along with the binder on the surface of the lactose particles and the initially formed agglomerates (Fig. 6b). This explains why the spray-on procedure causes a higher dissolution rate than the melt-in procedure for Rylo (Fig. 3).

EDX-mapping of cross sections of agglomerates (Fig. 7) confirmed the above-mentioned effects of the binder addition procedure on the distribution of Lu–X. For all the binders, the EDX-mapping showed a random distribution of Lu–X domains in agglomerates produced by the melt-in procedure. By the spray-on procedure, however, domains of Lu–X are mainly seen in the core of the agglomerates with poloxamer (Fig. 7b) as well as PEG, whereas domains mainly are seen in the surface of the agglomerates with Rylo (Fig. 7d). For the agglomerates produced with Gelucire, the EDX-mapping showed a random distribution of Lu–X domains by the spray-on procedure. This indicates that the lower viscosity of Gelucire compared with PEG and poloxamer (Table 4) results in more agglomerate formation by distribution, i.e. the immersion mechanism is less dominant. Accordingly, the effect of the binder addition procedure on the dissolution rate is less pronounced for Gelucire than for PEG and poloxamer (Fig. 3).

Seo et al. (2003) did not find any differences in the dissolution profile obtained from agglomerates produced in a high shear mixer by two different binder

addition procedures, melt-in and pump-on. This is supposed to be because of the more efficient mixing in the high shear mixer. A higher shearing force will promote distribution as the agglomerate formation mechanism.

4. Conclusions

The study showed that it was possible to produce agglomerates containing solid dispersions by melt agglomeration in a rotary processor. The binder addition procedure was found to influence the dissolution profile obtained from the agglomerates produced in the rotary processor.

Differences in the intragranular distribution of Lu–X could explain the different dissolution profiles from the agglomerates produced by the two binder addition procedures. Furthermore, the intragranular distribution of Lu–X could be explained by the mechanisms of agglomerate formation and growth. The melt-in procedure resulted in agglomerates with Lu–X distributed randomly in the agglomerates regardless of the mechanism. The spray-on procedure resulted in a higher content of Lu–X in the core of the agglomerates when the dominating mechanism was immersion and in a higher content of Lu–X at the periphery of the agglomerates when the dominating mechanism was distribution.

The solid dispersions formed by the melt agglomeration process were found to be stabile during storage for up to 12 weeks at 25 °C and 50% RH since the dissolution profiles obtained from the agglomerates did not change during this period.

Acknowledgement

Particle Analytical ApS is acknowledged for making the EDX-mapping possible.

References

Damian, F., Blaton, N., Naesens, L., Balzarini, J., Kinget, R., Augustijns, P., Van den Mooter, G., 2000. Physicochemical characterization of solid dispersions of the antiviral agent UC-781 with polyethylene glycol 6000 and Gelucire 44/14. Eur. J. Pharm. Sci. 10, 311–322.

Eliasen, H., Schæfer, T., Kristensen, H.G., 1998. Effects of binder rheology on melt agglomeration in a high shear mixer. Int. J. Pharm. 176, 73–83.

European Pharmacopoeia, 2002. European Pharmacopoeia, fourth ed. Council of Europe, Strasbourg, pp. 205–207.

Ford, J.L., Rubinstein, M.H., 1980. Formulation and ageing of tablets prepared from indomethacin-polyethylene glycol 6000 solid dispersions. Pharm. Acta Helv. 55, 1–7.

Gupta, M.K., Tseng, Y.-C., Goldman, D., Bogner, R.H., 2002. Hydrogen bonding with adsorbent during storage governs drug dissolution from solid-dispersion granules. Pharm. Res. 19, 1663–1672.

Khoo, S.-M., Porter, C.J.H., Charman, W.N., 2000. The formulation of Halofantrine as either non-solubilising PEG 6000 or solubilising lipid based solid dispersions: physical stability and absolute bioavailability assessment. Int. J. Pharm. 205, 65–78.

Kinget, R., Kemel, R., 1985. Preparation and properties of granulates containing solid dispersions. Acta Pharm. Technol. 31, 57–62.

McTaggart, C.M., Ganley, J.A., Sickmueller, A., Walker, S.E., 1984. The evaluation of formulation and processing conditions of a melt granulation process. Int. J. Pharm. 19, 139–148.

Passerini, N., Gonzalez-Rodriguez, M.L., Cavallari, C., Rodriguez, L., Albertini, B., 2002. Preparation and characterisation of ibuprofen-poloxamer 188 granules obtained by melt granulation. Eur. J. Pharm. Sci. 15, 71–78.

Schæfer, T., Johnsen, D., Johansen, A., 2004. Effects of powder particle size and binder viscosity on intergranular and intragranular particle size heterogeneity during high shear granulation. Eur. J. Pharm. Sci. 21, 525–531.

Schæfer, T., Mathiesen, C., 1996. Melt pelletization in a high shear mixer. IX. Effects of binder particle size. Int. J. Pharm. 139, 139–148.

Seo, A., Holm, P., Kristensen, H.G., Schæfer, T., 2003. The preparation of agglomerates containing solid dispersions of diazepam by melt agglomeration in a high shear mixer. Int. J. Pharm. 259, 161–171.

Serajuddin, A.T.M., 1999. Solid dispersion of poorly water-soluble drugs: early promises, subsequent problems, and recent breakthroughs. J. Pharm. Sci. 88, 1058–1066.

Serajuddin, A.T.M., Sheen, P.-C., Mufson, D., Bernstein, D.F., Augustine, M.A., 1988. Effect of vehicle amphiphilicity on the dissolution and bioavailability of a poorly water-soluble drug from solid dispersions. J. Pharm. Sci. 77, 414–417.

Vilhelmsen, T., Kristensen, J., Schæfer, T., 2004. Melt pelletization with polyethylene glycol in a rotary processor. Int. J. Pharm. 275, 141–153.

Voinovich, D., Moneghini, M., Perissutti, B., Filipovic-Grcic, J., Grabnar, I., 2000. Preparation in high-shear mixer of sustained-release pellets by melt pelletisation. Int. J. Pharm. 203, 235–244.

Zhou, F., Vervaet, C., Remon, J.P., 1996. Matrix pellets based on the combination of waxes, starches and maltodextrins. Int. J. Pharm. 133, 155–160.